ELSEVIER

Journal of Alloys and Compounds 446–447 (2007) 630–634

Journal of ALLOYS AND COMPOUNDS

www.elsevier.com/locate/jallcom

The effects of the substitution of Ti and La for Zr in $ZrMn_{0.7}V_{0.2}Co_{0.1}Ni_{1.2}$ hydrogen storage alloys on the phase structure and electrochemical properties

J.C. Sun*, S. Li, S.J. Ji

Institute of Materials and Technology, Dalian Maritime University, Dalian 116026, China

Received 12 October 2006; received in revised form 8 March 2007; accepted 22 March 2007
Available online 30 March 2007

Abstract

In this paper, phase structure and electrochemical properties of the overstoichiometric hydrogen storage electrode alloys $Zr_{1-x}Ti_x$ ($Mn_{0.7}V_{0.2}Co_{0.1}Ni_{1.2}$) have been investigated. The results showed that when the Ti content increased, the content of the C15 Laves phase decreased while that of the C14 Laves phase increased. At same time, the high Ti content inhibited the appearance of secondary phase Zr_7M_{10} in the alloys. When $x = 0.2$, the storage hydrogen electrode alloy $Zr_{0.8}Ti_{0.2}$ ($Mn_{0.7}V_{0.2}Co_{0.1}Ni_{1.2}$) possessed the maximum discharge capacity 354 mAh/g, and preserved 91% of total capacity at current 300 mA/g. Due to a few La additation, the alloy $Zr_{0.75}Ti_{0.2}La_{0.05}Mn_{0.7}V_{0.2}Co_{0.1}Ni_{1.2}$ reached the maximum capacity 372 mAh/g after 4 cycles, compared to 14 cycles for the alloy without La, and preserved 93% of the maximum capacity after 30 cycles.

Keywords: Zr-based Laves phase; ZrNi phase; Alloying; High rate dischargeability; Activation property

1. Introduction

The development of electric vehicle has been paid much more attentions for reducing the environmental pollution of exhaust emission in urban area. Nickel-metal hydride (Ni/MH) batteries using hydrogen storage alloys as the negative electrode have been developed and commercialized to meet strong market demand for portable power source. In the past decade, being used as an active material of negative electrode for Ni/MH battery, Zr-based AB_2 type Laves phase hydrogen storage alloys have been extensively investigated due to its higher theoretical charging–discharging capacity (~500 mAh/g) and good cycling durability. However, some issues, such as poor activate process, insufficient high rate dischargeability and discharging capacity, are still remained to be improved for the commercial application of electric vehicle. It is well known that multi-component substitution in alloys is an effective method to improve the electrochemical properties of hydrogen storage alloys and that a series of Zr-based AB_2 type stoichiometric multicomponent alloys have been derived and developed from binary ZrV_2, $ZrMn_2$ and $ZrCr_2$ [1–3]. It is reported that the introduction of non-stoichiometry into Zr-based Laves phase alloys does not change alloy's structure, but changes the lattice parameters slightly and their hydrogen storage properties considerably, such as plateau pressure, plateau slope and kinetics of sorption and electrochemical discharge capacity [4]. Furthermore, the introduction of rear earth element into Zr-based Laves alloys alters the activation behaviors [3]. For the Zr-based stoichiometric AB_2 alloys, some effects of the substitution of Ti for Zr on electrochemical performances of the alloys are strongly dependant on the alloy systems. Shu et al. [5] reported that the Ti substitution for $Zr(NiVMnCr)_2$ has no effect on the microstructure and the activation process, but can improve their discharge capacity and cycle life. Du et al. [6] found that the discharge capacity of $Zr_{1-x}Ti_x(NiVMnCo)_2$ alloys has the maximum value with increasing Ti content. In the Ti additive alloys system the high rate dischargeability had been improved and the cycle life was deteriorated with Ti content. In our previously reported alloy $Zr_{1-x}Ti_xCr_{0.4}Mn_{0.2}V_{0.1}Ni_{1.3}$ [7], Ti substitution ($x = 0.1$) for Zr in the alloys improves the discharge capacity and rate dischargeability. When $x > 0.1$, both activation and discharge capacity of $Zr_{1-x}Ti_xCr_{0.4}Mn_{0.2}V_{0.1}Ni_{1.3}$ ($x = 0.1$–0.3) alloys decrease.

* Corresponding author. Tel.: +86 411 84727959; fax: +86 411 84727959.
E-mail address: sunjc@dlmu.edu.cn (J.C. Sun).

0925-8388/$ – see front matter © 2007 Elsevier B.V. All rights reserved.
doi:10.1016/j.jallcom.2007.03.108

With Zr substituted by Ti in Zr-based AB_2 alloys, the discharge capacity of alloys can be improved because the atomic weight of Ti is less than that of Zr. Meanwhile, decreasing the stability of alloy hydride with substitution of Zr by Ti also results in the increase of the dynamic of hydrogen desorption of alloys. Both of stated factors are positive effect on the discharge capacity of the alloys. On the other hand, the volume of hydrogen storage interstitial site can be contracted because the radius of Ti atom is smaller than that of Zr atom. The electrochemical performances of the alloys may be closely related to the above factors. For the non-stoichiometric AB_2-type Laves phase alloys, the non-stoichiometry at different positions on Zr–Ti–Mn–Co–Ni and Zr–Ti–Mn–Co–Fe alloys has evidently changed the hydrogen storage properties and electrochemical performances [4,8]. So it is important to determine the substituted amounts of Zr element with Ti element in a specific alloy system and to clarify the effect of substitution Ti and La for Zr on the surface properties of the alloys.

In our previous works, the effects of substitution of Ti for Zr on structures and electrochemical properties were clarified and reported in the alloy $ZrCr_{0.4}Mn_{0.2}V_{0.1}Ni_{1.3}$ from Zr–Cr–Ni alloy system [7]. In the present study, the over-stoichiometric alloy $Zr(Mn_{0.7}V_{0.2}Co_{0.1}Ni_{1.2})$ as a parent alloy from Zr–Mn–Ni system was developed, which showed large hydrogen storage capacity. To improve its activation behavior and rate discharge-capability, the effects of the substitution of Ti and La for Zr in over-stoichiometric alloys $Zr(Mn_{0.7}V_{0.2}Co_{0.1}Ni_{1.2})$ on phase structure and electrochemical characteristic have been investigated.

2. Experimental

The alloys were synthesized from pure element 99.9% (except Mn 99.7%) by arc melting in an argon atmosphere. To ensure homogeneity, these alloys were remelted four times and mechanically pulverized in air and sieved to 275 meshes.

The hydride electrodes were prepared by cold pressing the mixtures of alloy powders with powdered electrolytic copper (200 mesh) in the weight ratio of 1:2 to form porous 10 mm diameter pellets in copper holders. Electrochemical charge–discharge tests were carried out in a standard open tri-electrode electrolysis cell, in which the counter electrode was nickel oxyhydroxide, the reference electrode was Hg/HgO/6 M KOH, and the electrolyte was 6 M KOH solution. The discharge capacities of hydride electrodes were determined by the galvanostatic charge–discharge method. The electrodes were fully charged at a current density of 100 mA g^{-1} for 6 h and discharged at 50 mA g^{-1} to the cut-off potential −0.6 V (versus Hg/HgO). The rate dischargeability can be defined as $HRDn = Cn/(Cn + C_{50}) \times 100\%$, where Cn is the discharge capacity under current densities (n mA/g), and C_{50} is the residual discharge capacity at 50 mA/g after the electrode potential fell to −0.6 V (versus Hg/HgO) under the discharge current of n mA/g. The HRD measurements are carried out after the alloy electrodes are fully activated.

Powder X-ray diffraction measurements were performed using a D/MAX-3A diffractometer with Co Kα radiation. The morphology of the alloys was observed in Philips XL-3 scanning electron microscopy (SEM), using the samples polished and then etched with a solution of 80 ml CH_3CH_2OH + 10 ml HCl + 10HF. Electron probe microanalysis (EPMA) (JCXA-733) was performed to identify the phases and the elemental distribution of the alloys.

3. Result and discussion

The X-ray diffraction patterns of the sample of $Zr_{1-x}Ti_x$ $(Mn_{0.7}V_{0.2}Co_{0.1}Ni_{1.2})$ with $x = 0.0$–0.5 are shown in Fig. 1. It can be seen that the parent alloy is consisted of cubic C15 Laves phase and minor second phase Zr_7Ni_{10}. With increasing Ti content, the intensity of diffraction peaks of C14 phase increases gradually and that of the second phase Zr_7Ni_{10} decreases and disappears entirely with $x > 0.3$. These results indicate that the abundance of hexagon C14 Laves phase increases and that of cubic C15 Laves phase and secondary phase (Zr_7Ni_{10}) decreases. Fig. 2 shows the SEM image of the alloys $Zr_{1-x}Ti_x$ $(Mn_{0.7}V_{0.2}Co_{0.1}Ni_{1.2})$. It can be seen that the C15 and C14 Laves phases are dendritic and second phases are segregated between arms of the dentrites. The dark and bright region corresponded to Laves phase (C15 and C14) and secondary phase Zr_7Ni_{10}. The results are in good agreement with that of the XRD analysis.

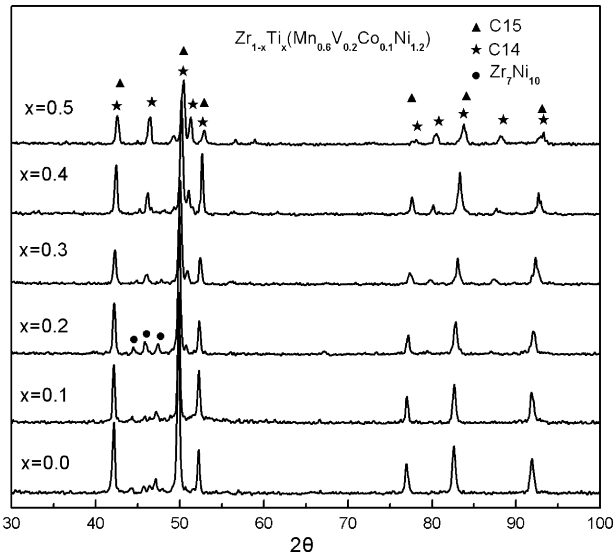

Fig. 1. XRD patterns of the alloys $Zr_{1-x}Ti_x$ $(Mn_{0.7}V_{0.2}Co_{0.1}Ni_{1.2})$.

Table 1 shows the lattice parameter and cell volume of the alloys $Zr_{1-x}Ti_x$ $(Mn_{0.7}V_{0.2}Co_{0.1}Ni_{1.2})$. It can be found that the lattice parameter and cell volume of both C15 and C14 decrease with the increasing Ti content. The results indicate the substitution of Ti for Zr atom lead to the shrinkage of cell volume of the alloys due to the smaller atomic radius of Ti than that of Zr. On the other hand, the results demonstrated Ti atoms enter into both C15 and C14 Laves phase at random, because the tendency of the cell volume shrinkage for both C15 and C14 is similar.

In order to further identify the composition of the alloys, we analyze surface composition of the alloys by means of EPMA.

Table 1
Lattice parameter and crystalline volume of the alloys $Zr_{1-x}Ti_x$ $(Mn_{0.7}V_{0.2}Co_{0.1}Ni_{1.2})$

Composition	C15		C14		
	a (nm)	V (nm^3)	a (nm)	c (nm)	V (cm^3)
$x = 0.0$	0.7037	0.3485			
$x = 0.1$	0.7025	0.3467			
$x = 0.2$	0.7014	0.3451	0.4960	0.8129	0.1732
$x = 0.3$	0.6993	0.3420	0.4950	0.8089	0.1717
$x = 0.4$	0.6945	0.3350	0.4935	0.8063	0.1701
$x = 0.5$	0.6939	0.3341	0.4912	0.8023	0.1676

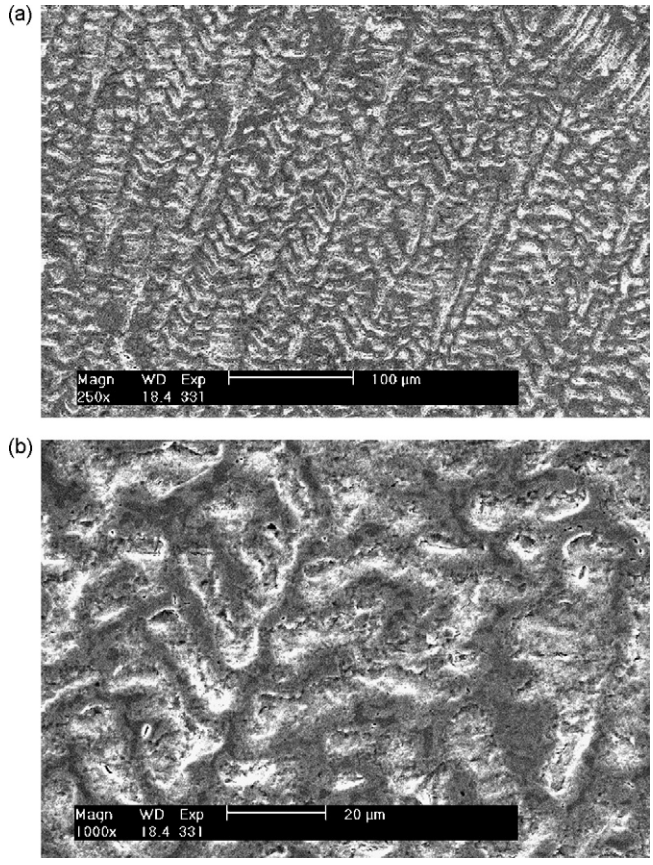

Fig. 2. SEM photograph of the alloy $Zr_{0.8}Ti_{0.2}$ ($Mn_{0.7}V_{0.2}Co_{0.1}Ni_{1.2}$) (a) 250×; (b) 1000×.

The nominal compositions of alloys are calculated and listed in the Table 2. For the parent $AB_{2.2}$ alloy, it is consisted of cubic C15 type Laves phase ($ZrMn_{0.76}V_{0.26}Co_{0.12}Ni_{1.3}$) and minor secondary phase Zr_7M_{10} ($ZrMn_{0.1}V_{0.01}Co_{0.03}Ni_{1.32}$). The C15 phase is corresponding to the formula $AB_{2.4}$ composition with more content of manganese compared to the nominal composition of parent alloy. With the increasing Ti content in $x = 0.1$–0.2, the abundance of the secondary phase (Zr_7M_{10} and TiNi) increase slightly. When $x = 0.4$–0.5, the alloys only consist of cubic C15 and hexagon C14 Laves phases without secondary

Table 2
The real composition of different phases in the alloys $Zr_{1-x}Ti_x$ ($Mn_{0.7}V_{0.2}Co_{0.1}Ni_{1.2}$)

Sample		Real composition
$x = 0.0$	Black	$ZrMn_{0.76}V_{0.26}Co_{0.12}Ni_{1.3}$
	White	$ZrMn_{0.1}V_{0.01}Co_{0.03}Ni_{1.32}$
$x = 0.1$	Black	$Zr_{0.93}Ti_{0.07}Mn_{0.73}V_{0.33}Co_{0.11}Ni_{1.4}$
	White	$(ZrMn_{0.15}V_{0.03}Co_{0.03}Ni_{1.19})$ $(TiNi)_{0.05}$
$x = 0.2$	Black	$Zr_{0.80}Ti_{0.20}Mn_{0\cdot70}V_{0.24}Co_{0.1}Ni_{1.3}$
	White	$ZrMn_{0.2}V_{0.4}Co_{0.01}Ni_{1.28}(TiNi)_{0.35}$
$x = 0.4$	Black	$Zr_{0.61}Ti_{0.39}Mn_{0.77}V_{0.32}Co_{0.11}Ni_{1.23}$
	White	$Zr_{0.6}Ti_{0.4}Mn_{0.57}V_{0.2}Co_{0.004}Ni_{1.15}$
$x = 0.5$	Black	$Zr_{0.52}Ti_{0.48}Mn_{0.56}V_{0.19}Ni_{1.33}$
	White	$Zr_{0.55}Ti_{0.45}Mn_{0.79}V_{0.35}Co_{0.03}Ni_{1.25}$

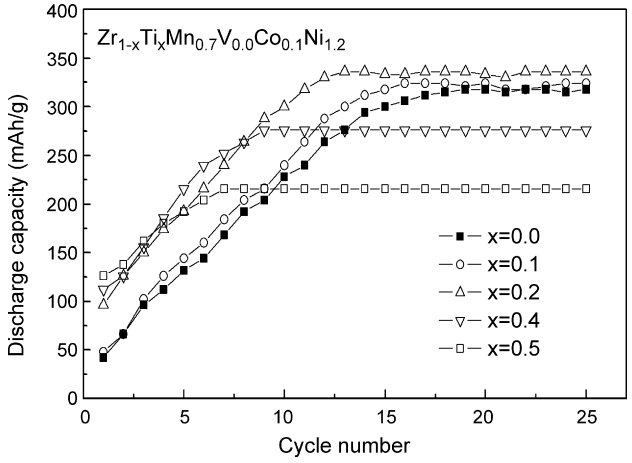

Fig. 3. Discharge capacity of hydride electrodes $Zr_{1-x}Ti_x$ ($Mn_{0.7}V_{0.2}Co_{0.1}Ni_{1.2}$) as a function of cycle number.

non-Laves phase, where Ti atoms are dispersed at random. These above results coincide with the results of XRD pattern.

Fig. 3 shows discharge capacity of hydrogen storage alloys as a function of cycle numbers. The discharge capacity of parent alloy exhibits maximum value 328 mAh/g at current density of 50 mA/g after 18 cycles. While the alloy with $x = 0.2$ reaches its maximum discharge capacity 354 mAh/g after 13 cycles. With the increasing the Ti content, the discharge capacity of the alloys decreases. The discharge capacity of alloy with $x = 0.5$ exhibits only 232 mAh/g. It should be noted that when the substitution of Ti for Zr increases, there is a maximum discharge capacity. It is well known that the discharge capacity of the alloy is not only relate to its hydrogen storage capacity but also its electrochemical kinetics of hydrogen discharging. Hout et al. [9] reported that C15 Laves phase in (Zr,Ti) (MNi) alloys could absorb a large amounts of hydrogen, while the C14 Laves phase exhibited better kinetics with a lower hydrogen storage capacity than that of C15 phase. When the substitution of Ti for Zr in the alloys increases, the content of C15 Laves phase decreases and that of C14 Laves phase increases. Although the total hydrogen storage capacity of the alloy is decreased, the electrochemical kinetics is improved. Furthermore, the substitution of Ti reduces the stability of the alloys and improves the surface electrocatalytic activity, which induces the hydrogen atom release easily. On the other hand, the secondary phase (Zr_7M_{10} and TiNi) may play an important role in the electrocatalytic activity. The parent alloy, which possesses better hydrogen storage capacity, exhibits lower discharge capacity due to surface poor electrocatalytic activity. Whereas the alloys with $x = 0.4$–0.5 also exhibit lower discharge capacity because of remarkable increase of C14 phase and evident decrease of the total hydrogen storage capacity. It is obviously noted that there should be an optimum Ti content in the alloys and that the alloy with $x = 0.2$ exhibits maximum discharge capacity 354 mAh/g.

Considering the activation process, it can also be seen that the activation behavior of the alloys is improved with the substitution of Ti and the activation cycling numbers reduce for all alloys with $x = 0.1$–0.5. These altering tendencies of activation behaviors with Ti substitution content in this work are contrary to

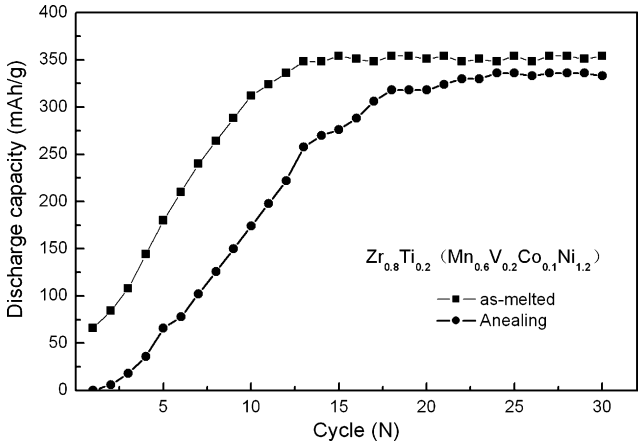

Fig. 4. The discharge capacity of $Zr_{0.8}Ti_{0.2}Mn_{0.6}V_{0.2}Co_{0.1}Ni_{1.2}$ alloy as a function of cycling numbers before and after annealing at 1373 K for 5 h.

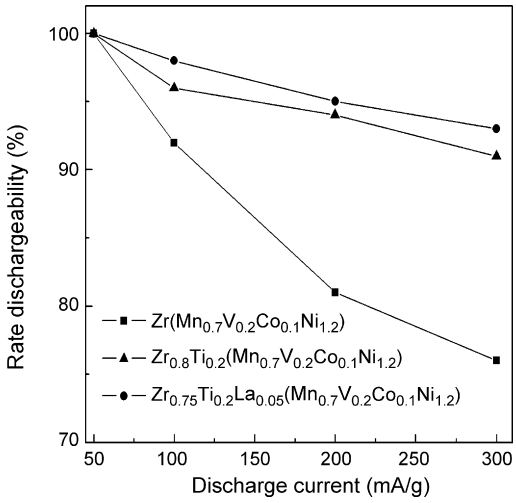

Fig. 5. The high-rate dischargeability of the electrode alloys $Zr_{1-x}Ti_x(Mn_{0.7}V_{0.2}Co_{0.1}Ni_{1.2})$.

our previously reported results for $Zr_{1-x}Ti_xCr_{0.4}Mn_{0.2}V_{0.1}Ni_{1.3}$ stoichiometric alloys, where the increase of Ti substitution content for Zr prolongs the activation cycling numbers [7]. In order to classifying the influence of secondary Zr–Ni phase on the discharging properties, the as-melted Ti-substituted alloy ($x = 0.2$) had been annealed in 1373 K for 6 h to homogenize composition and to diminish the secondary phase. After heat treatment, the secondary Zr–Ni phase in this work alloys is considerably diminished; the discharge capacity decreases and the activation cycling numbers increase, as shown in Fig. 4, which is coincided with the results reported by Vicintin et al. [10]. But Knosp et al. [11] reported that the secondary Zr–Ni phase does not alter the activation process. Since different results were obtained by using different composition alloys, hence, there are still other factors to influence on the activation process and discharging properties in addition to the secondary Zr–Ni phase. Generally, the activation process is controlled by the surface oxide feature of AB_2 alloys. And a dense surface oxide film leads to the poor activation behavior of the Zr-based hydride alloys. In this work, the substitution of Ti for Zr in Zr–Mn–Ni electrode alloy system with higher Mn and V content not only alters the quantity and dissolution of Mn, V and Zr oxides (as seen in Table 2, Mn and V is segregated on surface) and charge conductivity of surface oxide film, but also enhances the brittleness and easy cracking of the alloy, which is different from the Zr–Cr–Ni alloy system with lower Mn and V content in Ref. [7]. Therefore, the activation process of over-stoichiometric AB_2-type Laves phase alloys may be controlled and dominated by surface composition and phase structure simultaneously in a specific alloy system and alloy's composition.

The high rate dischargeability (HRD) of Ti-substituted alloys ($x = 0.0$–0.5) is closely related to the activation behaviors. Corresponding to $x = 2$, the specific alloy possesses a maximum HRD. Fig. 5 shows the of the electrode alloys $Zr(Mn_{0.7}V_{0.2}Co_{0.1}Ni_{1.2})$ and $Zr_{0.8}Ti_{0.2}(Mn_{0.7}V_{0.2}Co_{0.1}Ni_{1.2})$. It can be seen that the discharge capacity of the parent alloy Exhibits 76% of the maximum capacity (50 mA/g) at the current 300 mA/g, while the discharge capacity of alloy can show 91% of the maximum capacity (50 mA/g) at the same condition. From above XRD results, it can be found that there are C15 and C14 Laves phases coexisting with amounts of second phase (Zr_7M_{10} and TiNi) in both alloys. As increasing Ti substitution for Zr in $x = 0.0$–0.2, the more C14 Laves phase and second phase (Zr_7M_{10} and TiNi) with a better electrocatalytic activity [12] enhance the HRD. However, in $x = 0.3$–0.5, more Ti substitution for Zr deteriorates the HRD. The above results also prove that the effects of Ti substitution for Zr should be considered as the synergistic function of each phase in the alloy and surface state.

In order to improve the activation behaviors further, a small amount of La was added into the alloy $Zr_{0.8}Ti_{0.2}(Mn_{0.7}V_{0.2}Co_{0.1}Ni_{1.2})$, whose surface morphology was shown in Fig. 6. It is seen from the micrograph that much micro-cracks and some caves on the surface occurred with multi-phase structure. These micro-cracks and caves will provide the alloys with a good activation property. The activation cycling number of La-added alloy $Zr_{0.75}Ti_{0.2}La_{0.05}(Mn_{0.7}V_{0.2}Co_{0.1}Ni_{1.2})$ was decreased to four cycles with maximum discharge capacity of 372 mAh/g, compared to the alloy $Zr_{0.8}Ti_{0.2}(Mn_{0.7}V_{0.2}Co_{0.1}Ni_{1.2})$ of 14 cycles with 354 mAh/g (Fig. 7). The high rate discharge-

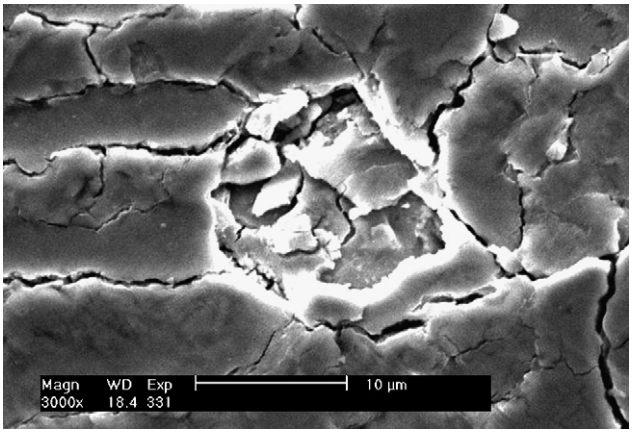

Fig. 6. SEM image of the alloy $Zr_{0.75}Ti_{0.2}La_{0.05}$ $(Mn_{0.7}V_{0.2}Co_{0.1}Ni_{1.2})$.

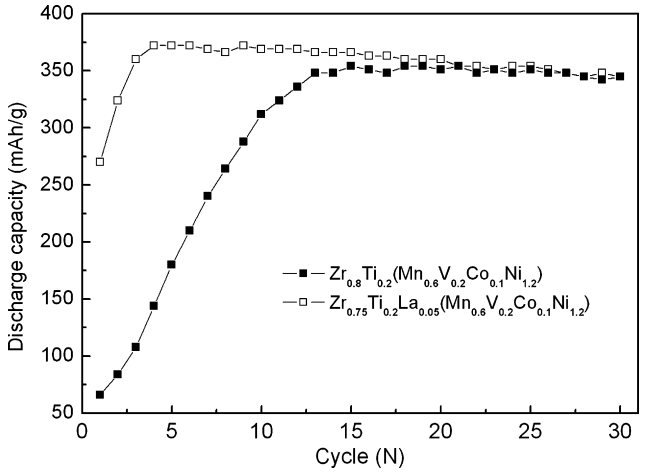

Fig. 7. the discharge capacities of $Zr_{0.8}Ti_{0.2}(Mn_{0.6}V_{0.2}Co_{0.1}Ni_{1.2})$ and $Zr_{0.75}Ti_{0.2}La_{0.05}(Mn_{0.6}V_{0.2}Co_{0.1}Ni_{1.2})$ alloys vs. cycling number.

ability is improved (as shown in Fig. 5). After 30 cycle of charge–discharge, the 93% of maximum capacity still remains. This results show that the substitution of La for Zr in $Zr_{0.8}Ti_{0.2}(Mn_{0.7}V_{0.2}Co_{0.1}Ni_{1.2})$ alloy has enhanced the activation performances, discharge capacity and HRD.

4. Conclusion

With increasing substitution of Ti for Zr, the content of cubic C15 Laves phase and that of hexagonal C14 Laves phase of the alloys $Zr_{1-x}Ti_x$ $(Mn_{0.7}V_{0.2}Co_{0.1}Ni_{1.2})$ decreases and increase, respectively. It has been found that there is minor second phase, such as Zr_7M_{10} and TiNi, in the alloys with $x = 0.1$–0.2. However, the minor second phase disappears entirely for the alloys with $x = 0.4$–0.5. After substitution of Ti for Zr, the Ti atoms are dispersed into C15 and C14 Laves phase of the alloys at random, which induce the shrinkage of lattice parameter of both Laves phase simultaneously. The substitution of a small amount of Ti for Zr is effective to improve the discharge capacity, rate capability. The alloy exhibits the most discharge capacity 354 mAh/g after 13 cycles and preserves 91% of the maximum capacity at the current density of 300 mA/g. As a few La substitution, the alloy $Zr_{0.75}Ti_{0.2}La_{0.05}Mn_{0.7}V_{0.2}Co_{0.1}Ni_{1.2}$ reached the maximum capacity 372 mAh/g after four cycles, compared to 14 cycles for the alloy without La, and preserved 93% of the maximum capacity after 30 cycles.

References

[1] M. Bououdina, P. Menier, J.L. Soubeyroux, D. Fruchart, J. Alloys Compd. 253/254 (1997) 302–307.
[2] S.M. Lee, Ho. Lee, J.H. Kim, et al., J. Alloys Compd. 308 (2000) 259.
[3] M. Dalin Sun, A. Latroche, Guégan-Percheron, J. Alloys Compd. 248 (1997) 215.
[4] M. Kandavel, S. Ramaprabhu, J. Alloys Compd. 381 (2004) 140–150.
[5] K. Su, S. Zhang, Y. Lei, J. Alloys Compd. 349 (2003) 237.
[6] Y.L. Du, X.G. Yang, Q.A. Zhang, et al., Int. J Hydrogen Energy 26 (2001) 333.
[7] J.C. Sun, S. Li, S.J. Ji, J. Alloys Compd. 404–406 (2005) 687.
[8] M. Kandavel, S. Ramaprabhu, J. Phys. Condens. Matter 15 (2003) 7501.
[9] J. Huot, E. Akiba, Y. Ishido, J. Alloys Compd. 231 (1995) 85–89.
[10] A. Visintin, H.A. Peretti, F. Ruiz, H.L. Corso, W.E. Triaca, J. Alloys Compd. 428 (2007) 244–251.
[11] B. Knosp, C. Jordy, Ph. Blanchard, T. Berlureau, J. Electrochem. Soc. 145 (1998) 1478–1482.
[12] D.M. Kim, K.J. Jang, J.Y. Lee, J. Alloys Compd. 293–295 (1999) 583–592.